ELSEVIER

CYTOKINE

www.elsevier.com/locate/issn/10434666

Cytokine ■■ (2005) ■■■–■■■

Lack of tumor necrosis factor receptor type 1 inhibits liver fibrosis induced by carbon tetrachloride in mice

Kaori Sudo[a,*], Yasuhiro Yamada[b], Hisataka Moriwaki[b], Kuniaki Saito[a], Mitsuru Seishima[a]

[a]*Department of Informative Clinical Medicine, Gifu University Graduate School of Medicine, 1-1 Yanagido, Gifu 501-1194, Japan*
[b]*First Department of Internal Medicine, Gifu University Graduate School of Medicine, 1-1 Yanagido, Gifu 501-1194, Japan*

Received 10 August 2004; received in revised form 16 November 2004; accepted 17 November 2004

Abstract

Chronic liver injury causes liver regeneration, resulting in fibrosis. The proinflammatory cytokine tumor necrosis factor (TNF) is involved in the pathogenesis of many acute and chronic liver diseases. TNF has pleiotropic functions, but its role in liver fibrosis has not been clarified. Chronic repeated injection of CCl_4 induces liver fibrosis in mice. We examined whether signaling through TNF receptors was critical for this process, using mice lacking either TNF receptor (TNFR) type 1 or TNFR type 2 to define the pathophysiologic role of TNFR signals in liver fibrosis. Liver fibrosis caused by chronic CCl_4 exposure was TNF-dependent; histological fibrosis was seen in wild-type (WT) and TNFR-2 knockout (KO) mice, but not in TNFR-1 KO mice. Furthermore, a marked reduction in procollagen and TGF-β synthesis was observed in TNFR-1 KO mice, which also had little detectable NF-κB, STAT3, and AP1 binding, and reduced levels of liver interleukin-6 (IL-6) mRNA compared to WT and TNFR-2 KO mice. In conclusion, our results indicate the possibility that NF-κB, STAT3, and AP1 binding by signals transduced through TNFR-1 plays an important role in liver fibrosis formation.

Keywords: Liver fibrosis; Tumor necrosis factor; Transcription factors; Interleukin-6; Transforming growth factor-β

1. Introduction

TNF acts by binding to type 1 or type 2 receptors (TNFR-1 and TNFR-2, respectively) and most of its effects on various cells are mediated primarily through TNFR-1 and TNFR-2, which function as the main transducers for membrane-anchored (non-soluble) TNF [1,2]. TNF is a pleiotropic cytokine involved in inflammation and immunity and is considered to be a proinflammatory cytokine in inflammation, liver injury, and cell death/apoptosis [1]. Increased TNF levels in the liver are seen after exposure to certain chemicals and in acute and chronic liver disease [2]. Chronic liver injury frequently causes liver fibrosis, resulting in liver cirrhosis [3–5]. Despite many efforts to clarify the pathogenesis of liver fibrosis, the molecular and cellular mechanisms of the disease have not been clearly elucidated. CCl_4 is a hepatotoxin that causes direct hepatocyte injury by altering the permeability of the plasma, lysosomal, and mitochondrial membranes. In hepatocytes, highly

Abbreviations: CCl_4, carbon tetrachloride; KO, knockout; NF-κB, nuclear factor κB; TGF-β, transforming growth factor-β; TNF, tumor necrosis factor; TNFR, tumor necrosis factor receptor; EMSA, electrophoretic mobility shift assay; mRNA, messenger RNA; RT-PCR, reverse-transcription polymerase chain reaction; AP1, activator protein 1; ICAM-1, intracellular adhesion molecule 1; VCAM-1, vascular cell adhesion molecule 1; STAT3, signal transducers and activator of transcription 3; C/EBP, CCAAT/enhancer binding protein; cDNA, complementary DNA.

* Corresponding author. Tel.: +81 58 230 6430; fax: +81 58 230 6431.

E-mail address: kaorin-s@cc.gifu-u.ac.jp (K. Sudo).

1043-4666/$ - see front matter © 2004 Elsevier Ltd. All rights reserved.
doi:10.1016/j.cyto.2004.11.001

reactive free radicals are also formed by the mixed function oxidase system during CCl_4 metabolism, causing severe centrilobular necrosis [6,7]. Recently, it has been shown that CCl_4 causes not only primary liver necrosis, but also hepatocyte apoptosis [1,8]. CCl_4-induced liver injury is also associated with increased levels of cytokines, including TNF, which is thought to enhance CCl_4-mediated injury [9]. In CCl_4-induced liver inflammation, TNF regulates inflammatory cell influx and induces the expression of other cytokines and adhesion molecules [8]. In liver regeneration after CCl_4 injury, TNF is important for hepatocyte proliferation, acting as a mitogen. TNFR-1 KO mice show deficient liver regeneration [2,10]. In liver fibrosis, the role of TNF acting through TNFR-1 and TNFR-2 has not been clarified. One important question is whether signaling through TNFR-1 or TNFR-2 is required for the regulation of liver fibrosis induced by CCl_4.

2. Results

2.1. Changes in liver histopathology and plasma ALT levels after CCl_4 injection

Typical photomicrographs of acute CCl_4-induced inflammatory and fibrotic changes in the liver are shown in Fig. 1 (H&E staining) and Fig. 2 (Azan staining). No differences were observed in the inflammatory cell infiltrate in the three groups (Fig. 1A, B and C). After CCl_4 treatment, plasma ALT levels increased to the same extent in WT and TNFR-1 and TNFR-2 knockout mice (WT mice vs. TNFR-1 KO mice or TNFR-2 KO mice, $p = 0.599$ or $p = 0.834$, respectively; TNFR-1 KO mice vs. TNFR-2 KO mice, $p = 0.78$) (Fig. 1D). However, Azan staining, which indicates collagen deposition around Glisson's sheath, was significantly weaker in TNFR-1 KO mice (Fig. 2B) than in the other two groups (Fig. 2A and C). The collagen area determined by densitometric analysis of the Azan staining results, was plotted (Fig. 2D). Fibrosis area in TNFR-1 KO mice was significantly reduced compared to that in WT ($^*p < 0.05$) and TNFR-2 KO mice ($^*p < 0.05$). No significant difference was observed in fibrosis area between WT and TNFR-2 KO mice. Three pathologists confirmed each histopathologic change. Livers from sham treated mice of each type showed no evidence of fibrosis (not shown). These findings indicated that TNFR-1 regulates liver fibrosis after CCl_4 treatment.

2.2. Expression of ICAM-1 and VCAM-1 mRNAs in WT and TNFR-1 and TNFR-2 KO mice treated with CCl_4

As shown in Fig. 3, after CCl_4 treatment, no differences were seen among the three groups in ICAM-1

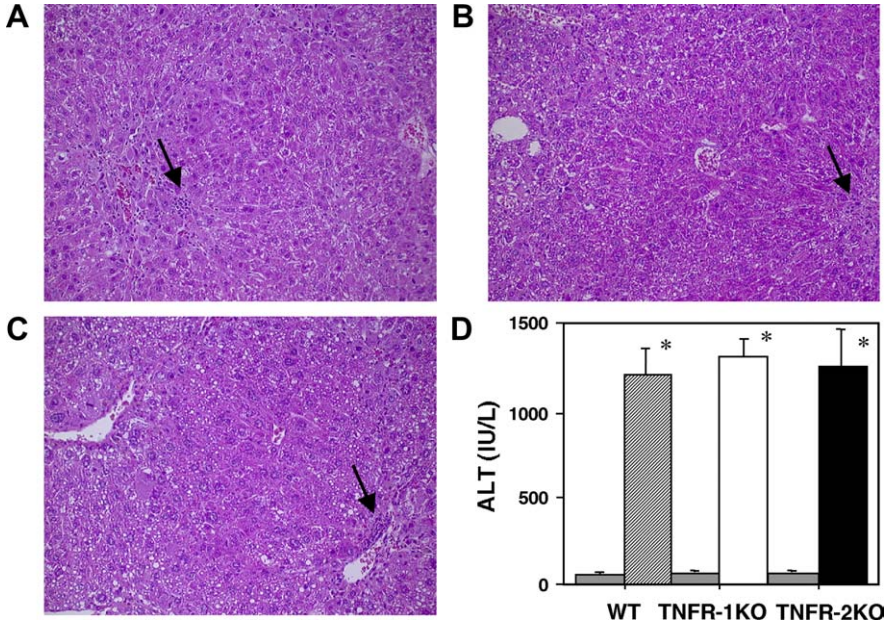

Fig. 1. Liver morphology and the effect of CCl_4 on plasma ALT activity after CCl_4 administration in WT and TNFR-1 and TNFR-2 KO mice. WT and TNFR-1 and TNFR-2 KO mice were injected intraperitoneally twice a week for 4 weeks with CCl_4 (1.0 ml/kg body weight). Liver tissue from WT mice (A), TNFR-1 KO mice (B), or TNFR-2 KO mice (C) was stained with hematoxylin–eosin. Liver samples from at least 10 animals were examined; the results shown are representative. The areas of inflammatory cell infiltrate are indicated (by the arrow). Magnification, ×400. Plasma was obtained from at least 10 animals, and ALT levels were determined as described in Section 4. In each group, the left bar (gray) indicates untreated mice, while the right bar (diagonal lines, unfilled, and filled) indicates CCl_4-treated mice (D, the bars indicate the ± SD of the means. $^*p < 0.05$ compared to the untreated animals).

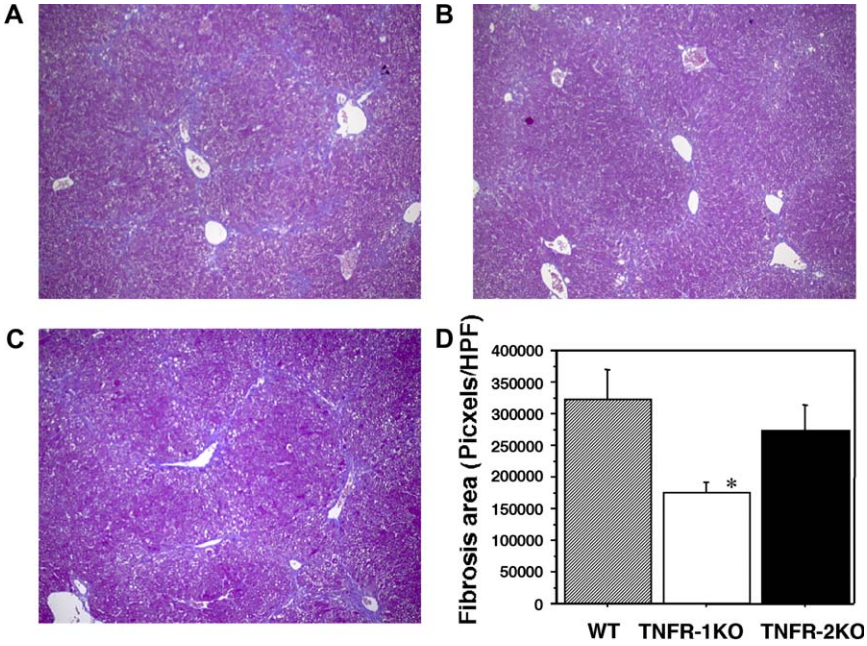

Fig. 2. Histological detection of collagen in the liver using Azan staining. Liver tissue from WT mice (A) and TNFR-1 KO mice (B) and TNFR-2 KO mice (C) taken after 4 weeks of CCl_4 treatment was stained with Azan solution. Blue staining indicates the presence of collagen. At least 10 animals were examined; the results shown are representative. Magnification, ×400. The collagen area of blue staining, determined by NIH Image analysis (NIH Image 1.61) of the results of Azan staining, was plotted (D, $n = 4$, the bars indicate the ± SD of the means).

mRNA levels (WT mice vs. TNFR-1 or TNFR-2 KO mice, $p = 0.391$ or $p = 0.107$, respectively; TNFR-1 KO mice vs. TNFR-2 KO mice, $p = 0.413$) or VCAM-1 mRNA levels (WT mice vs. TNFR-1 or TNFR-2 KO mice, $p = 0.468$ or $p = 0.418$, respectively; TNFR-1 KO mice vs. TNFR-2 KO mice, $p = 0.113$).

2.3. Expression of TGF-β2 and procollagen α1 (I) mRNA in WT and TNFR-1 and TNFR-2 KO mice treated with CCl_4

In WT and TNFR-2 KO mice, repeated injection of CCl_4 resulted in the appearance of fibrous tissue in proximity to the vena centralis, as revealed by Azan staining of collagen. This histological change was markedly reduced in TNFR-1 KO mice (Fig. 2). Procollagen α1 (I) gene expression has been employed as an early marker of tissue fibrosis, and correlates with the degree of CCl_4-induced liver fibrosis in mice. The CCl_4-induced increase in the procollagen α1 (I) mRNA level, measured by RT-PCR, was lower in TNFR-1 KO mice than in the other two groups (Fig. 4B). TGF-β2, a profibrogenic and proliferation factor for hepatic stellate cells involved in collagen synthesis, is also commonly used to assess fibrotic responses [11]. Following repeated CCl_4 administration, TGF-β2 expression in the liver was increased in WT and TNFR-2 KO mice, but not in TNFR-1 KO mice (Fig. 4C).

2.4. Liver IL-6 mRNA levels in WT and TNFR-1 and TNFR-2 KO mice after CCl_4 administration

To determine whether the hepatic IL-6 mRNA level is lower in TNFR-1 KO mice than in WT and TNFR-2 KO mice, we measured IL-6 expression in the liver and found that, following repeated CCl_4 administration, the IL-6 mRNA level was significantly lower in TNFR-1 KO mice than in WT and TNFR-2 KO mice (Fig. 5).

2.5. Binding of transcription factors

EMSA was used to analyze the binding of various transcription factors, NF-κB, STAT3, AP1, and C/EBP, in liver nuclear extracts from WT and TNFR-1 and TNFR-2 KO mice. Since TNF stimulates NF-κB activation in normal and chemical injury in the liver [2]. Absence of TNFR-1 signaling after CCl_4 administration completely abolishes binding of NF-κB, STAT3 and AP1. Binding of NF-κB heterodimer p50/65 in extracts of WT and TNFR-2 KO mice became detectable after 4 weeks CCl_4 administration. In contrast, p50/65 NF-κB binding was not detectable in nuclear extracts of TNFR-1 KO mice. In the same way as binding of NF-κB, binding of STAT3 and AP1 was also not detectable in TNFR-1 KO mice, whereas binding of C/EBP was detectable in all group mice. The binding of the four transcription factors was assessed by super shift analysis with specific antibodies (data not shown). The absence

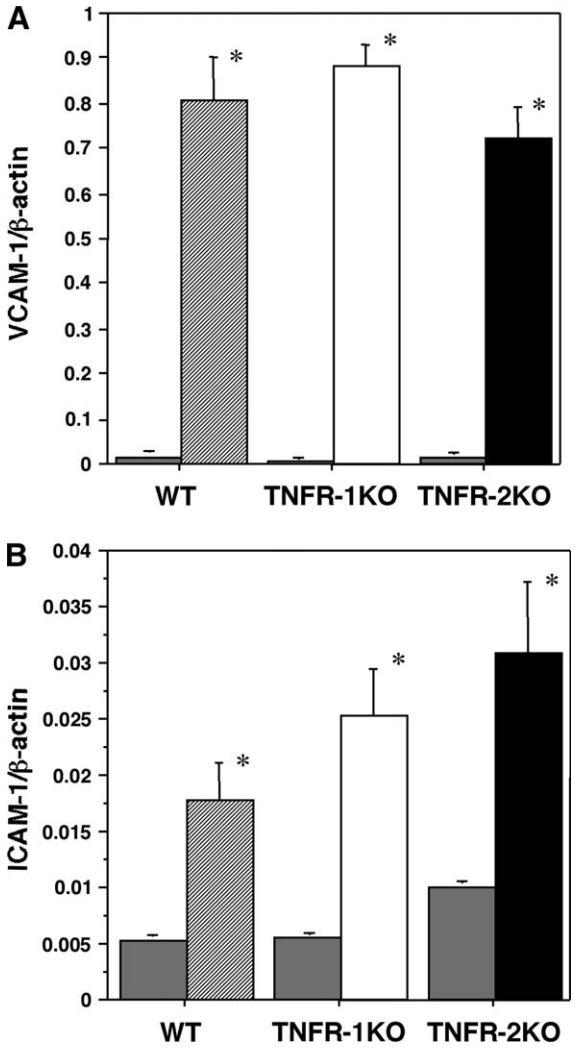

Fig. 3. Expression of adhesion molecule mRNAs in the liver of WT and TNFR-1 and TNFR-2 KO mice after CCl_4 administration. The levels of VCAM-1 mRNA (A) and ICAM-1 mRNA (B) were measured using the real-time PCR assay. Each value was normalized to β-actin expression in the same samples and presented as a fold-increase compared to the control value. In each group, the left bar (gray) indicates untreated mice, while the right bar (diagonal lines, unfilled, and filled) indicates CCl_4-treated mice (The bars indicate the ± SD of the means. *$p < 0.05$ compared to untreated animals).

of a functional TNFR-1 was found to interfere with the binding of NF-κB, STAT3, and AP1, but not C/EBP (Fig. 6).

3. Discussion

Liver fibrosis may be caused by many events, including viral infection, alcoholism, and autoimmune diseases. In liver injury, many cytokines are involved in regeneration and fibrosis. Several methods have been developed to produce liver fibrosis in animals [12–14]. Chronic intermittent administration of CCl_4 induces fibrotic changes after marked infiltration of the inflammatory cells, especially mononuclear cells, such as neutrophils, thus mimicking the changes seen in chronic viral hepatitis-associated fibrosis, and has therefore been widely used to experimentally induce liver fibrosis and cirrhosis. In addition to its cytotoxic effects, CCl_4 activates several transcription factors [2,15], including NF-κB [16], a transcription factor complex with an essential role in the expression of adhesion molecules and several inflammatory cytokines, including IL-6 [17]. CCl_4 toxicity is thought to be mediated by at least two sequential processes. The first involves the cytochrome P450-mediated metabolism of CCl_4 to a highly reactive trichloromethyl radical, which initiates lipid peroxidation and leads to hepatocellular membrane damage. This is followed by the release of inflammatory mediators from the activated hepatic macrophages, which are thought to potentiate CCl_4-induced hepatic injury. TNF is a pleiotropic proinflammatory cytokine produced rapidly by macrophages in response to tissue injury. Since CCl_4-induced liver injury is associated with high levels of TNF [2], we examined the effect of TNF signaling through TNF receptors on liver fibrosis using KO mice lacking either TNFR-1 or TNFR-2. Our results clearly showed that liver fibrosis in TNFR-1 KO mice was much reduced compared to that in WT or TNFR-2 KO mice, as demonstrated by a decreased intensity of Azan staining and a decreased level of intrahepatic collagen α1 (I) mRNA. These results suggest that TNF is an essential mediator of CCl_4-induced hepatic fibrosis.

We also measured plasma ALT levels and evaluated liver injury by H&E staining in the three groups of mice. Although the ALT level increased markedly after CCl_4 treatment, indicating hepatocyte damage, in all the three groups, there was no difference in ALT levels among the groups. Histological studies showed infiltration of mononuclear cells around the Glisson's sheath after 4 weeks of CCl_4 treatment.

The central role of TNF in up-regulating ICAM-1 and VCAM-1 expression, thereby promoting adhesion of leukocytes to, and transmigration through, the endothelial barrier, is well documented [18]. Following CCl_4 administration, ICAM-1 and VCAM-1 expression increased, as demonstrated by real-time PCR, but to the same extent in all the three groups after 4 weeks. Hence, it is likely that cytokines other than TNFα regulate the expression of adhesion molecules in liver fibrosis. However, the expression of adhesion molecules in liver within 15 h following CCl_4 administration was decreased in TNFR-1 KO mice, but was unaffected in WT or TNFR-2 KO mice [8].

TGF-β2, one of the fibrogenic factors involved in collagen synthesis, is also commonly used to assess fibrotic responses [11,13]. In chronic inflammation or necrosis, TGF-β2 increases fibroblast proliferation, and

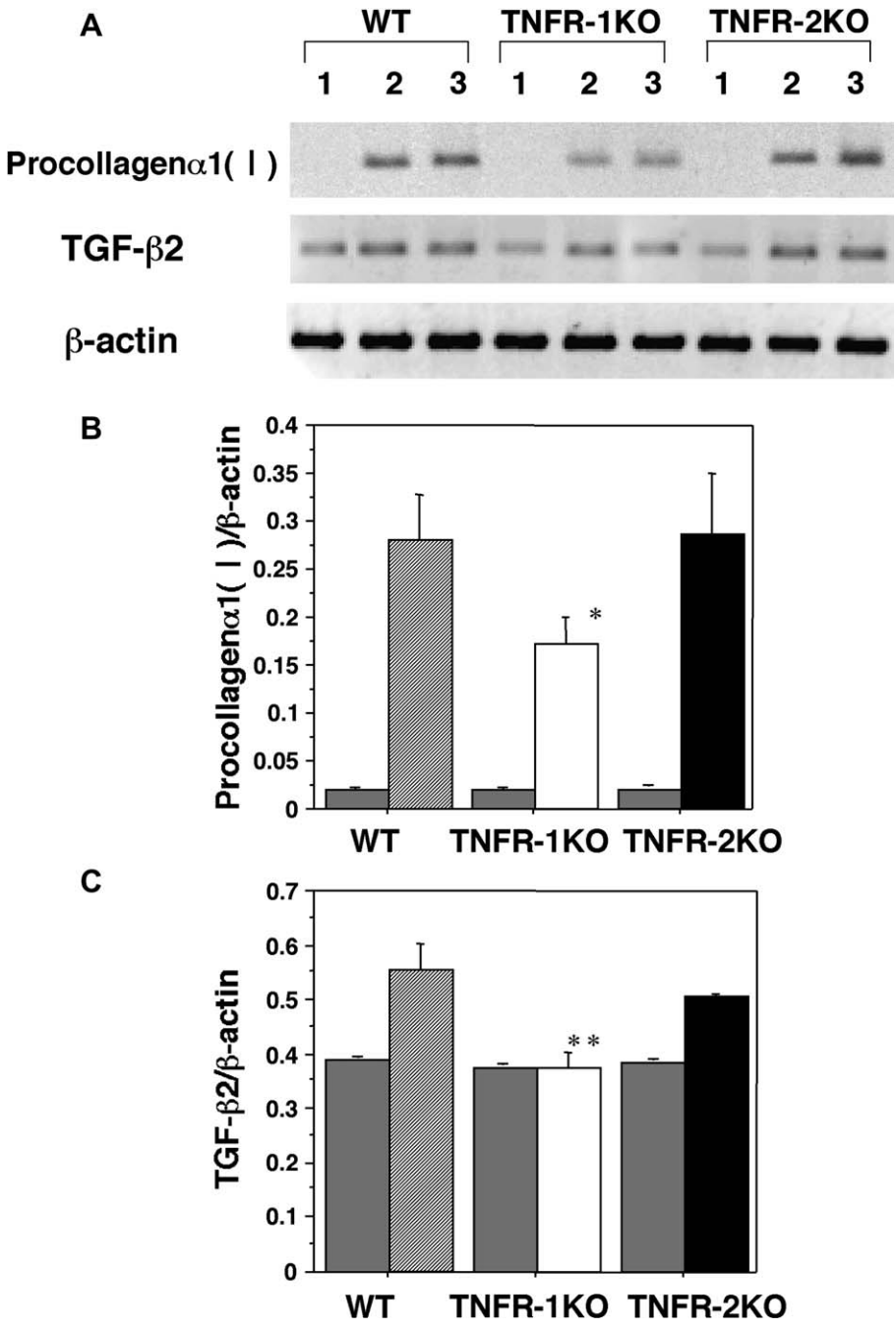

Fig. 4. Procollagen α1 (I) and TGF-β2 mRNA levels in the liver of WT and TNFR-1 and TNFR-2 KO mice before and after CCl_4 administration. RNA was obtained from the liver of control and CCl_4-treated WT and TNFR-1 and TNFR-2 KO mice (see Section 4) and the levels of procollagen α1 (I) mRNA and TGF-β2 mRNA were measured using the reverse transcriptase PCR assay. (A), ethidium bromide-stained 1.5% agarose gels of PCR products. Lane 1 represents CCl_4-untreated mice, lanes 2, 3 represent CCl_4-treated mice. (B), procollagen α1 (I) mRNA and (C), TGF-β2 mRNA levels were normalized to the β-actin mRNA level in the same samples ($n = 4$, the bars indicate the means ± SD) and presented as a fold-increase compared to the control value. The level of each mRNA in TNFR-1 KO mice was significantly suppressed compared to those in WT and TNFR-2 KO mice (*$p < 0.05$ and **$p < 0.01$).

the increased number of fibroblasts results in increased production of extracellular matrix molecules, such as collagen and fibronectin [5]. TGF-β2 initiates signaling through the ligand-dependent activation of a complex of heteromeric transmembrane/serine threonine kinases, consisting of type 1 (R1) and type 2 (R2) TGF-β receptors [19]. Activated TGF-β R1 receptors then phosphorylate and thus activate Smad2 and/or Smad3, two signaling mediators of the SMAD protein family [20,21]. Through this signaling pathway, TGF-β induces the expression of extracellular matrix molecules such as collagen α1 (I). The present study

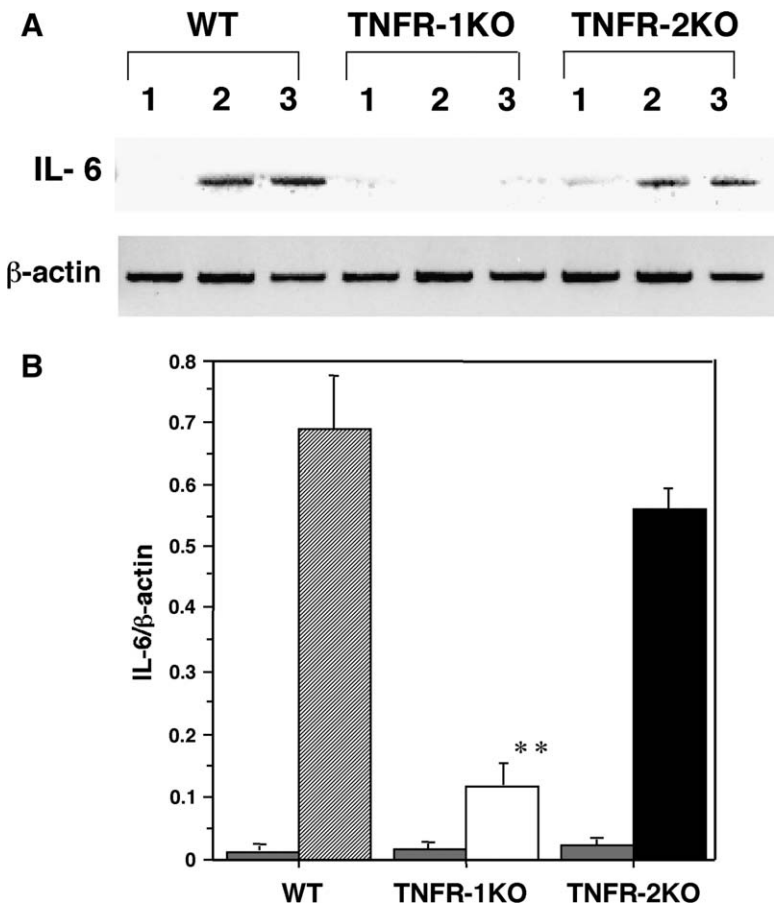

Fig. 5. IL-6 mRNA levels in the livers of WT and TNFR-1 and TNFR-2 KO mice before and after CCl_4 administration. RNA was obtained from the livers of CCl_4-injected WT and TNFR-1 and TNFR-2 KO mice (see Section 4) and IL-6 mRNA levels measured using the reverse transcriptase PCR assay. (A), ethidium bromide-stained 1.5% agarose gels of PCR products. Lane 1 represents CCl_4-untreated mice, lanes 2, 3 represent CCl_4-treated mice. (B), IL-6 mRNA levels normalized to the β-actin mRNA level in the same sample ($n = 4$, the bars indicate the means ± SD). The level of IL-6 mRNA in TNFR-1 KO mice was significantly suppressed compared to that in WT (**$p < 0.01$) and TNFR-2 KO (**$p < 0.01$) mice. No significant difference was observed in the fibrosis area between WT and TNFR-2 KO mice.

showed that the CCl_4-induced increase in TGF-β2 expression seen in the liver of WT and TNFR-2 KO mice was completely suppressed in TNFR-1 KO mice, showing that TNF-mediated induction of TGF-β2 is mediated by TNFR-1. Blockage of the TNFR-1 signaling pathway also resulted in a striking reduction in collagen deposition and a smaller increase in collagen α1 (I) gene expression following CCl_4 administration. Taken together, these results show that the absence of the TNFR-1 signaling pathway resulted in reduced collagen deposition and a smaller increase in TGF-β2 and collagen α1 (I) gene expression.

TNF plays an important role in the induction of liver fibrosis by CCl_4 exposure, and signal transduction through TNFR-1 on the liver cell membrane is critical for liver fibrosis. After CCl_4 injury, NF-κB, STAT3, and AP1 binding was seen in WT and TNFR-2 KO mice, but not in TNFR-1 KO mice. We therefore predict that NF-κB and STAT3 regulate TGF-β2 levels through TNFR-1 signaling. In a liver fibrosis model, fibrotic changes are less evident in IL-6 KO mice than in WT mice [22]. Moreover, CCl_4-induced expression of TGF-β and collagen deposition in the liver is significantly reduced in IL-6 KO mice [23]. IL-6 may function downstream of TNF in ameliorating liver injury and liver fibrosis [22]. In CCl_4-induced liver fibrosis, IL-6 is considered to be an essential mediator [23], because it also stimulates STAT3 activation [2,24]. We have previously shown that hepatic IL-6 mRNA levels are increased by CCl_4 injection and that IL-6 is induced by NF-κB signaling [2].

The present study provides evidence that the suppression of liver fibrosis in TNFR-1 KO mice is due to the lack of signaling through TNFR-1. We conclude that NF-κB, STAT3, and AP1 binding, are all involved in liver fibrosis formation. These results not only lead to better understanding of the mechanisms controlling collagen expression by cytokines as the TNF but also provide a molecular basis for antifibrotic effect of NF-κB, STAT3, and AP1 binding by signals transduced through TNFR-1, which is helpful for the treatment of liver fibrosis.

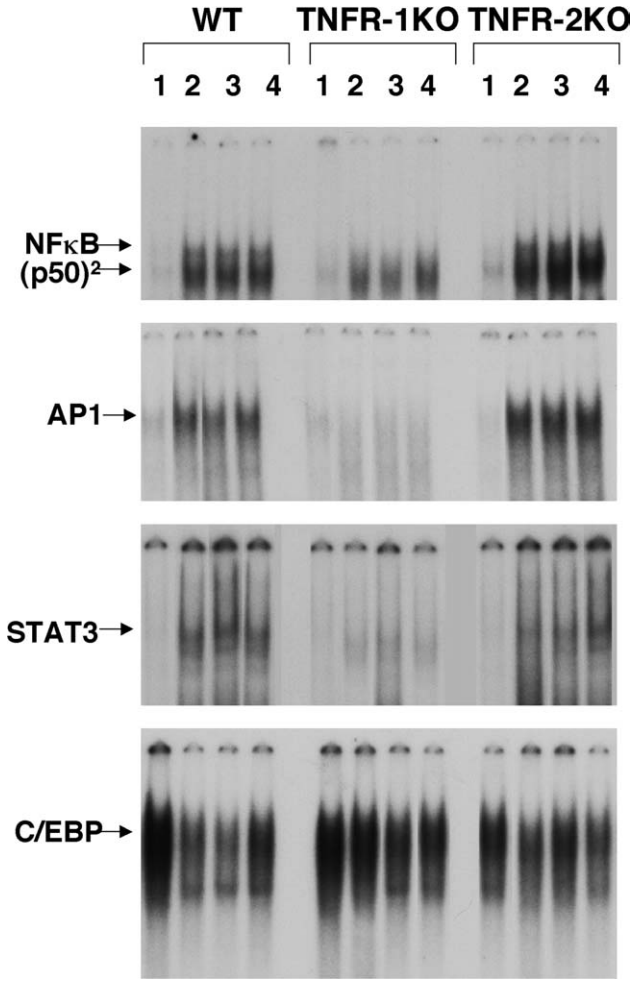

Fig. 6. NF-κB, STAT3, AP1, and C/EBP binding in CCl_4-induced liver fibrosis. WT and TNFR-1 and TNFR-2 KO mice were killed 48 h after the final CCl_4 injection. A liver nuclear extract was then prepared and EMSA performed with 10 μg of nuclear protein and 0.2 ng of ^{32}P-end-labeled double-stranded oligonucleotide probes for NF-κB, STAT3, AP1, and C/EBP as described in Section 4. p50 homodimer and p50/65 heterodimer are indicated as $(p50)^2$ and NF-κB, respectively. Lane 1 represents CCl_4-untreated mice ($n = 1$), lanes 2, 3 and 4 represent CCl_4-treated mice ($n = 3$). The same liver nuclear extract was used to detect NF-κB, STAT3, AP1, and C/EBP binding.

4. Materials and methods

4.1. Animals and treatments

TNFR-1 KO mice (p55−/− p75+/+), developed in the C57BL/6 strain, and TNFR-2 KO mice (p55+/+p75−/−), in which the mutation has been moved onto a C57BL/6 background by five successive backcrosses, were used [24]. WT C57BL/6 mice, purchased from Jackson Laboratories (Bar Harbor, ME), served as controls. All experiments were performed using male mice weighing 20–25 g kept in a temperature-controlled room with an alternating 12-h dark and light cycle. The animal experiments were conducted in accordance with the institutional guidelines of the Gifu University School of Medicine. At least 10 mice were used in each experiment. We also have done the same experiments at least 3 different times with different samples from those in this study. Mice were injected intraperitoneally twice a week for 4 consecutive weeks with 1 ml/kg body weight of CCl_4 (Sigma, St. Louis, MO) diluted 1:20 in olive oil (total volume injected 20 ml/kg body weight), then were sacrificed 48 h after the last injection. One part of the liver was frozen in liquid nitrogen and stored at −80 °C until used for RNA extraction, while another was fixed in 4% buffered paraformaldehyde for 18–24 h and paraffin embedded. Blood samples were obtained by cardiac puncture and drawn into glass tube containing 7.5% EDTA (pH 7.4). The plasma was immediately separated by centrifugation and stored at 4 °C.

4.2. ALT activity

Alanine transaminase (ALT) levels were determined using a HITACHI model 7600 (HITACHI, Ibaraki, Japan).

4.3. Nuclear extracts

Liver tissue was homogenized and nuclear extracts prepared as described previously [24], then frozen and stored at −80 °C until use. All solutions used for the preparation of nuclear extracts contained protease inhibitors [24]. Protein concentrations were measured using the Bradford method (Bio-Rad Laboratories, Richmond, CA) with bovine serum albumin as the standard.

4.4. Electrophoretic mobility shift assay (EMSA)

The double-stranded DNA probe used for NF-κB, AP1, and C/EBP was a consensus oligonucleotide probe from Santa Cruz Biotechnology (Santa Cruz, CA), while that used for STAT3 was an oligonucleotide corresponding to the binding site for the Sis inducible factor (Santa Cruz Biotechnology, Santa Cruz, CA). The probes were end-labeled with γ^{32}P-ATP using T4 polynucleotide kinase (Invitrogen Life Technologies, U.S.A). A mixture of 10 μg of nuclear protein and 0.2 ng of ^{32}P-end-labeled double-stranded oligonucleotide probe [24] was incubated for 30 min at room temperature, then electrophoresed on a 5% polyacrylamide Tris-glycine-EDTA gel. The gels were dried and exposed to Kodak (Rochester, NY) X-AR film for a period of 2 h–2 days at −80 °C.

4.5. RNA extraction from liver tissue and determination of gene expression by the reverse-transcription polymerase chain reaction and real-time PCR assay

Samples of liver tissue (approximately 30 mg) were homogenized and total RNA was extracted using the

ISOGEN RNA isolation kit (Nippon Gene, Tokyo, Japan). One microgram of total RNA was used for the synthesis of cDNA. RT-PCR was performed using a TaKaRa mRNA Selective PCR kit (TaKaRa Biomedicals, Tokyo, Japan). The sequences of the oligonucleotide primers were: β-actin, sense 5′-ATGGATGACGATATCGCT-3′ and antisense 5′-ATGAGGTAGTCTGTCAGGT-3′; TGF-β2, sense 5′-CCCCCGGAGGTGATTTCCAT-3′ and antisense 5′-TGGGGTTTTGCAAGCGGAAG-3′; α1 (I) procollagen, sense 5′-GAGCGGAGAGTACTGGATCG-3′ and antisense 5′-TGCTGTAGGTGAAGCGACTG-3′ (based on the sequence from Genbank accession no. U03419) [25]; IL-6, sense 5′-TTCCCTACTTCACAAGTCCGGAGA-3′ and antisense 5′-GACTCCAGCTTATCTGTTAGGAG-3′. The PCR products were visualized by ultraviolet illumination after electrophoresis for 30 min at 100 V through 1.5% agarose gels (COSMO BIO, Tokyo, Japan) and staining in Tris-borate/EDTA buffer containing 0.5 μg/ml of ethidium bromide. The signal intensity of the bands with the expected size was measured using an image analyzer (Bio-Profile system; M & S Instruments Trading Inc). Several PCR products were analyzed by real-time PCR using the SYBR Green PCR method and a Light Cycler sequence detector (Hoffmann-LaRoche Ltd., Basel, Switzerland). The sequences of the oligonucleotide primers were: β-actin, sense 5′-TGTTACCAACTGGGACGACATCG-3′ and antisense 5′-TCGGAACCGCTCGTTGCC-3′; ICAM-1, sense 5′-GGAAGGGAGCCAAGTAACTGT-3′ and antisense 5′-CTAAAGGCATGGCACACGTATG-3′; VCAM-1, sense 5′-CCTCACTTGCAGCACTACGGGCT-3′ and antisense 5′-TTTTCCAATATCCTCAATGACGGG-3′. Two microliters of the reverse-transcribed mixture was used in a PCR reaction performed according to the instructions provided with the CYBR Green PCR kit. The fluorescence intensity of each target gene was normalized to that of β-actin amplified under identical conditions.

4.6. Histology

The livers were fixed in 4% buffered paraformaldehyde for 18–24 h, and then the fixed tissues were embedded in paraffin, cut into 6 μm sections, and placed on Super frost-Plus microscope slides (Matsunami Glass Ind., Ltd). For immunohistochemical analysis, paraffin-embedded tissues were deparaffinized and dehydrated by sequential immersion in xylene, absolute ethanol, 80% ethanol, and PBS. Slides were stained with hematoxylin-eosin (H&E) or Azan solution for blind histopathological assessment. The slides were visualized on a Nikon microscope (ECLIPSE E800, Nikon Corporation, Tokyo, Japan) using a digital imaging system (FUJIX Digital Camera HC-300Zi, Nikon Corporation, Tokyo, Japan). NIH Image 1.61 was used to calculate the area of collagen deposition in fibrotic liver from video micrograph tiff files of 4× fields. The fibrosis ratio was also checked by three independent pathologists.

Acknowledgments

We appreciate the technical assistance of N. Furuta, A. Morise, S. Maeda, H. Ota and H. Ohashi. We also wish to thank Mr. Tom Barkas for proofreading the English of this manuscript.

References

[1] Baker SJ, Reddy EP. Transducers of life and death: TNF receptor superfamily and associated proteins. Oncogene 1996;12:1–9.
[2] Yamada Y, Fausto N. Deficient liver regeneration after carbon tetrachloride injury in mice lacking type 1 but not type 2 tumor necrosis factor receptor. Am J Pathol 1998;152:1577–89.
[3] Loreal O, Clement B, Schuppan D, Rescan PY, Rissel M, Guillouzo A. Distribution and cellular origin of collagen VI during development and in cirrhosis. Gastroenterology 1992;102:980–7.
[4] Hatahara T, Seyer JM. Isolation and characterization of a fibrogenic factor from CCl(4)-damaged rat liver. Biochim Biophys Acta 1982;716:377–82.
[5] Pierce RA, Glaug MR, Greco RS, Mackenzie JW, Boyd CD, Deak SB. Increased procollagen mRNA levels in carbon tetrachloride-induced liver fibrosis in rats. J Biol Chem 1987;262:1652–8.
[6] Slater TF. Necrogenic action of carbon tetrachloride in the rat: a speculative mechanism based on activation. Nature 1966;209:36–40.
[7] Shi J, Aisaki K, Ikawa Y, Wake K. Evidence of hepatocyte apoptosis in rat liver after the administration of carbon tetrachloride. Am J Pathol 1998;153:515–25.
[8] Simeonova PP, Gallucci RM, Hulderman T, Wilson R, Kommineni C, Rao M, et al. The Role of tumor necrosis factor-alpha in liver toxicity, inflammation, and fibrosis induced by carbon tetrachloride. Toxicol Appl Pharmacol 2001;177:112–20.
[9] Czaja MJ, Xu J, Alt E. Prevention of carbon tetrachloride-induced rat liver injury by soluble tumor necrosis factor receptor. Gastroenterology 1995;108:1849–54.
[10] Yamada Y, Webber EM, Kirillova I, Peschon JJ, Fausto N. Analysis of liver regeneration in mice lacking type 1 or type 2 tumor necrosis factor receptor: requirement for type 1 but not type 2 receptor. Hepatology 1998;28:959–70.
[11] Battegay EJ, Raines EW, Seifert RA, Bowen-Pope DF, Ross R. TGF-beta induces bimodal proliferation of connective tissue cells via complex control of an autocrine PDGF loop. Cell 1990;63:515–24.
[12] Tsukamoto H, Matsuoka M, French SW. Experimental models of hepatic fibrosis: a review. Semin Liver Dis 1990;10:56–65.
[13] Armendariz-Borunda J, Seyer JM, Postlethwaite AE, Kang AH. Kupffer cells from carbon tetrachloride-injured rat livers produce chemotactic factors for fibroblasts and monocytes: the role of tumor necrosis factor-alpha. Hepatology 1991;14:895–900.
[14] Kitamura K, Nakamoto Y, Akiyama M, Fujii C, Kondo T, Kobayashi K, et al. Pathogenic roles of tumor necrosis factor receptor p55-mediated signals in dimethylnitrosamine-induced murine liver fibrosis. Lab Invest 2002;82:571–83.
[15] Perez Tamayo R. Is cirrhosis of the liver experimentally produced by CCl4 and adequate model of human cirrhosis? Hepatology 1983;3:112–20.

[16] Liu SL, Degli Esposti S, Yao T, Diehl AM, Zern MA. Vitamin E therapy of acute CCl4-induced hepatic injury in mice is associated with inhibition of nuclear factor kappa B binding. Hepatology 1995;22:1474–81.
[17] Kopp EB, Ghosh S. NF-kappa B and rel proteins in innate immunity. Adv Immunol 1995;58:1–27.
[18] Vassalli P. The pathophysiology of tumor necrosis factors. Annu Rev Immunol 1992;10:411–52.
[19] Derynck R, Feng XH. TGF-beta receptor signaling. Biochim Biophys Acta 1997;1333:F105–50.
[20] Heldin CH, Miyazono K, ten Dijke P. TGF-beta signalling from cell membrane to nucleus through SMAD proteins. Nature 1997;390:465–71.
[21] Hoodless PA, Wrana JL. Mechanism and function of signaling by the TGF beta superfamily. Curr Top Microbiol Immunol 1998; 228:235–72.
[22] Kovalovich K, DeAngelis RA, Li W, Furth EE, Ciliberto G, Taub R. Increased toxin-induced liver injury and fibrosis in interleukin-6-deficient mice. Hepatology 2000; 31:149–59.
[23] Natsume M, Tsuji H, Harada A, Akiyama M, Yano T, Ishikura H, et al. Attenuated liver fibrosis and depressed serum albumin levels in carbon tetrachloride-treated IL-6-deficient mice. J Leukoc Biol 1999;66:601–8.
[24] Yamada Y, Kirillova I, Peschon JJ, Fausto N. Initiation of liver growth by tumor necrosis factor: deficient liver regeneration in mice lacking type I tumor necrosis factor receptor. Proc Natl Acad Sci U S A 1997;94:1441–6.
[25] Ikejima K, Honda H, Yoshikawa M, Hirose M, Kitamura T, Takei Y, et al. Leptin augments inflammatory and profibrogenic responses in the murine liver induced by hepatotoxic chemicals. Hepatology 2001;34:288–97.